Patient-Specific Dosimetry of Indium-111- and Yttrium-90-Labeled Monoclonal Antibody CC49

Peter K. Leichner, Gamal Akabani, David Colcher, Katherine A. Harrison, William G. Hawkins, Miriam Eckblade, Janina Baranowska-Kortylewicz, Samuel C. Augustine, James Wisecarver and Margaret A. Tempero
Departments of Radiology, Radiation Oncology, Pathology/Microbiology, Internal Medicine and Academic Computing Service, University of Nebraska Medical Center, Omaha, Nebraska

The objective of this work was to develop patient-specific dosimetry for patients with metastatic gastrointestinal tract cancers who received ^{111}In-CC49 IgG for imaging before therapy with ^{90}Y-CC49 IgG. **Methods:** Whole-body imaging of 12 patients, who received 111–185 MBq (3–5 mCi) of ^{111}In-CC49, commenced in < 2 hr postinfusion and was continued daily for 4–5 days. SPECT data were acquired at 24 and 72 hr to determine the range of ^{111}In-CC49 activity concentrations in tumors and normal organs. Time-activity curves were generated from the image data and scaled from ^{111}In-CC49 to ^{90}Y-CC49 for dosimetric purposes. Absorbed-dose calculations for ^{90}Y-CC49 included the mean and range in tumor and normal organs. Computed ^{90}Y-CC49 activity concentrations were compared with measurements on 10 needle biopsies of normal liver and four tumor biopsies. **Results:** In 9 of 10 normal liver samples, the range of computed ^{90}Y-CC49 activity concentrations bracketed measured values. This was also the case for 3 of 4 tumor biopsies. Absorbed-dose calculations for ^{90}Y-CC49 were based on patients' images and activities in tissue samples and, hence, were patient-specific. **Conclusion:** For the radiolabeled antibody preparations used in this study, quantitative imaging of ^{111}In-CC49 provided the data required for ^{90}Y-CC49 dosimetry. The range of activities in patients' SPECT images was determined for a meaningful comparison of measured and computed values. Knowledge of activity distributions in tumors and normal organs was essential for computing mean values and ranges of absorbed dose and provided a more complete description of the absorbed dose from ^{90}Y-CC49 than was possible with planar methods.

Key Words: dosimetry; monoclonal antibody; radioimmunotherapy

J Nucl Med 1997; 38:512–516

Iodine-131-labeled monoclonal antibodies (MAbs) B72.3 and CC49 that target the TAG-72 antigen have been investigated extensively for potential improvements in tumor diagnosis and treatment (*1–3*). No therapeutic efficacy has been shown in a Phase I trial with ^{131}I-CC49 in metastatic colon cancer with administered activities of up to 90 mCi/m^2 (*2*) and a Phase II trial in metastatic colon cancer with administered activities of 75 mCi/m^2 (*3*). In a subsequent Phase I trial, conducted at this center, 14 patients with various metastatic gastrointestinal tract cancers were treated with ^{131}I-CC49 using administered activities of up to 300 mCi/m^2. Although there was excellent localization of ^{131}I-CC49 in disease sites, there were no major tumor responses even at the highest administered activities.

The principal purpose of the present work is to report patient-specific dosimetry for ^{90}Y-labeled monoclonal antibody (^{90}Y-CC49) based on quantitative imaging of ^{111}In-CC49, tissue biopsies and serial blood samples. The clinical outcomes (toxicity and tumor response to treatment) will be reported in a separate publication. The development and clinical use of ^{90}Y-CC49 was based in part on the rationale that because of their higher energy, ^{90}Y beta particles produce higher initial absorbed-dose rates and more uniform absorbed-dose distributions than ^{131}I beta particles. In view of the demonstrated ability of MAb CC49 to target gastrointestinal tract adenocarcinomas, it was decided to undertake a Phase I trial with escalating administered activities of ^{90}Y-CC49. An additional practical consideration was that the administration of ^{90}Y-CC49 could be performed on an outpatient basis.

A difficulty associated with intravenously administered ^{90}Y-labeled antibodies is that they cannot be imaged quantitatively. Therefore, we have used ^{111}In-CC49 for quantitative imaging before the administration of ^{90}Y-CC49 for therapy. In making radiation absorbed-dose estimates for ^{90}Y-CC49, it was assumed that the ^{90}Y and ^{111}In preparations had the same tissue distributions. This assumption was validated by comparing computed activity concentrations of ^{90}Y-CC49 in the liver and several tumors with the results of activity measurements on needle biopsies. The dosimetry in this report is patient-specific because no standard masses or standard configurations of normal organs were assumed in making radiation absorbed-dose estimates. Instead, SPECT was used to determine activity distributions of ^{111}In-CC49 in all tumors and normal organs that had quantifiable localization by SPECT imaging. In particular, care was taken to determine not only mean values of activity concentrations but also maxima and minima in sets of transverse SPECT slices that bracketed tumors and normal organs. The results of this study suggest that this approach is important in comparing computed and measured activity concentrations. The determination of mean values and ranges of activity concentrations was also used to compute mean values and ranges of absorbed doses. As previously discussed, knowledge of the range of absorbed doses may be of importance in gaining a better understanding of normal-tissue toxicity and tumor response to radioimmunotherapy (RIT) (*4,5*).

MATERIALS AND METHODS

Patients

Twelve patients with measurable metastatic gastrointestinal tract carcinomas were studied. Patients ranged in age from 45 to 65 yr (median 52 yr). There were 6 women and 6 men. Underlying cancer diagnoses included pancreas (4 patients), colorectal (6 patients), esophagus (1 patient) and cholangiocarcinoma (1 patient). This Phase I study was approved by the Institutional Review Board of this institution and by the Cancer Therapy Evaluation Program of the National Cancer Institute. Informed consent was obtained from all patients. Patients underwent CT examinations before and after ^{90}Y-CC49 therapy to identify measurable disease. All CT examinations were evaluated by experienced radiologists familiar with the patients' medical history. Patients were administered escalating activities of ^{90}Y-CC49 as follows: five patients received 11.1 MBq/kg (0.3 mCi/kg), four patients received 14.8

Received Apr. 5, 1996; revision accepted Aug. 12, 1996.
For correspondence or reprints contact: Janina Baranowska-Kortylewicz, PhD, University of Nebraska Medical Center, Dept. of Radiation Oncology, Omaha, NE 68198-1050.

MBq/kg (0.4 mCi/kg) and three patients received 18.5 MBq/kg (0.5 mCi/kg). Total administered activities ranged from 640 MBq–1421 MBq (17.3 mCi–38.4 mCi).

Antibody Labeling and Radiolabeled Antibody Administration

Chelate conjugates of CC49 with N-[4-(4-isothiocyanatophenyl)-1-carboxypropyl-1,4,7,10-tetraazacyclododecane]-N′,N″,N‴-triacetic acid (PA-DOTA) (*6,7*) were stored at −70°C in sterile 2-ml, metal-free plastic vials that had been sealed with shrink-wrap tubing. All immunoconjugates were tested for immunoreactivity, sterility, lack of pyrogens and general safety. The storage vial was used for the radiolabeling reaction.

Indium-111 Labeling. An aliquot of $^{111}InCl_3$ in 0.05 *M* HCl was added to approximately 1 mg of the CC49-PA-DOTA chelate-conjugate in 0.2 ml ammonium acetate buffer, pH 6.5. An additional amount of nonradioactive $InCl_3$ in 0.5 *M* HCl was added to produce a molar ratio 2:1 of DOTA to In. The mixture was incubated at 37°C for 30 min. The reaction was terminated by the addition of diethylenetriaminepentaacetic acid (DTPA) and checked for incorporation using instant thin-layer chromatography (ITLC) plates. The labeled protein was separated from low molecular weight compounds by size exclusion chromatography using Sephadex G-50 (1.5 × 30 cm) (Sigma, St. Louis, MO) equilibrated with 0.05 *M* phosphate buffered saline (PBS). The ^{111}In-labeled CC49-PA-DOTA fraction was collected through a 0.2-μm filter into a sterile vial, assayed in a dose calibrator, tested for lack of pyrogens and the radiochemical purity was determined by ITLC before the administration to patients. The labeled MAb was also tested for sterility, and high-performance liquid chromatography (HPLC) was used to test for the presence of aggregates. Specific activities of approximately 185 MBq (5 mCi) per mg of IgG were routinely achieved for clinical preparations with ^{111}In.

Yttrium-90 Labeling. Yttrium-90 labeling was achieved by using ^{90}Y in 0.05 *M* HCl at 37°C in a similar manner to the ^{111}In labeling using approximately 4 mg of CC49-PA-DOTA chelate-conjugate. Specific activities of 185–555 MBq (5–15 mCi) per mg of IgG were routinely achieved for clinical preparations with ^{90}Y. The radiolabeled antibody construct was purified on a sterile Sephadex G-50 column (1.5 × 30 cm) using 0.05 *M* PBS. The product was filtered through a sterile 0.2-μm filter into the final labeled product vial, and a sample was removed for endotoxin testing. The radiolabeled antibody was diluted with human serum albumin (final HSA concentration was 1%) to minimize radiolysis. Samples for sterility, unit volume assay and binding assays were aseptically removed from the final activity container. Radiochemical purity was checked by ITLC and HPLC.

Patient Administration. The selected activity of radiolabeled CC49 IgG was diluted to 25 ml of saline containing 1% human serum albumin. The radiolabeled MAb was administered over 15 min and followed by a 25-ml flush of normal saline infused over 15 min. Although the labeled protein amounts were different for the ^{111}In-CC49 and ^{90}Y-CC49 administrations, the total administered protein was kept constant at 5 mg for each administration by adding unlabeled CC49.

Imaging and Radiation Dosimetry for Tumors and Normal Organs

Whole-body planar gamma camera and regional SPECT imaging of the chest and abdomen were used to generate the data required for tumor and normal organ dosimetry. Whole-body imaging commenced in less than 2 hr following the administration of ^{111}In-CC49 and was repeated at 24, 48 and 72 hr. Administered activities of ^{111}In-CC49 ranged from 111–185 MBq (3–5 mCi). SPECT acquisitions for the quantitation of activity in tumors and normal organs were performed at 24 and 72 hr postadministration.

TABLE 1
Effective Half-Life (hr) of Indium-111-CC49 in Tumors and Normal Tissues

Patient no.	Tumor		Liver		Spleen		Blood	
	T_α	T_β	T_α	T_β	T_α	T_β	T_α	T_β
1	67	—	12	67	67	—	1.1	63
2	NA*	—	25	52	71	—	3.1	60
3	47	—	12	60	—	—	3.8	42
4	68	—	22	68	66	—	3.8	42
5	NA*	—	8.0	68	68	—	2.8	60
6	37	—	6.0	83	58	—	2.7	40
7	43	—	24	68	67	—	3.3	48
8	41	—	11	65	48	—	4.6	61
9	5.5	68	5.5	68	64	—	4.8	32
10	NA*	—	24	62	62	—	5.9	52
11	60	—	8.0	90	78	—	2.3	53
12	6.0	75	6.0	75	6.0	75	6.0	34

*Not available; tumor uptake was too low for quantitation by noninvasive imaging.

All images were acquired on a dual-headed gamma camera system, equipped with medium-energy collimators. Energy windows of 15%, centered on the two photopeaks of ^{111}In, were used in all planar and tomographic image acquisitions. SPECT acquisitions were performed in 360° orbits, and images were acquired in 3° intervals at 30 sec per view. These planar projection data were acquired in 128^2 matrices.

The raw tomographic data were reconstructed using the circular harmonic transform (CHT) algorithm for quantitative SPECT (*8*) that has been validated in phantom studies (*9*) and in a study of radiolabeled antibody activity in the livers of beagle dogs (*10*). Reconstructed transverse slices, 1 pixel in thickness (4.67 mm), were stored in 128^2 matrices. The analysis of whole-body images was performed using the gamma camera system's computer software for generating ROIs. This analysis yielded relative clearance curves for ^{111}In-CC49 in tumors and normal organs. Reconstructed SPECT slices were analyzed volumetrically for absolute quantitation of activity concentration in tumors and normal organs using ROI computer software developed by our group. ROIs in SPECT slices were in most cases generated by setting a threshold as a fraction of the global maximum in a set of transverse slices that bracketed a tumor or normal organ. In some cases, ROIs were generated manually because of low tumor uptake. In all cases, ROIs were kept as tight as anatomically possible. ROIs in contiguous slices formed volumes of interest (VOIs), and the ^{111}In-CC49 activity in VOIs was determined using a gain factor for tomographic reconstruction (*9*). This gain factor was used to convert counts per voxel to activity per milliliter. The system was calibrated quarterly. The computer software provided total activity in a given volume as well as a mean value and maximum and minimum values of activity per milliliter.

The information about the distribution of ^{111}In-CC49 activity in the two SPECT reconstructions was used to convert relative clearance curves, obtained from whole-body images, to absolute clearance curves (kBq/g, μCi/g). Radiation absorbed-dose estimates for ^{90}Y-CC49 were generated from these data by scaling from the administered activity of ^{111}In-CC49 to that of ^{90}Y-CC49. Absorbed-dose estimates were thus based on SPECT volume determinations, the scaled ^{90}Y-CC49 concentration in each VOI, the average beta-particle energy of ^{90}Y (*11*) and the measured effective half-lives given in Table 1. Tumor and normal organ volumes in this investigation were large compared to the r_{90} distance (0.517 cm) of ^{90}Y beta particles (*11*). Therefore, boundary

effects were neglected and absorbed-dose calculations were made for complete absorption of ^{90}Y beta-particle energy. Additionally, all absorbed-dose calculations were made for complete biological removal and physical decay using the measured effective half-lives.

Blood Samples and Tissue Biopsies

In clinical trials, radiation absorbed-dose estimates for red marrow are usually based on the activity in whole blood as a function of time postinjection. Blood samples were drawn at 5 min, 30 min, 1 hr, 2 hr, 4 hr, 24 hr, 48 hr, 72 hr, 94 hr, 120 hr and 168 hr after the administration of ^{90}Y-CC49. The concentration of ^{90}Y-CC49 in these samples was measured in a well scintillation NaI(Tl) counter that had been calibrated with a ^{90}Y standard, obtained from the National Institute for Science and Technology. When measuring the activity of ^{90}Y-CC49 in blood samples, channels ranging in energy from 511 keV to 2000 keV, were used on the gamma counter. For these high-energy settings there was no contamination of counting rates from ^{111}In-CC49 that was also present in these samples. As discussed elsewhere (*12,13*), absorbed-dose estimates for red marrow based on the activity in blood samples require a reduction factor for blood to account for the difference in activity concentration in blood and marrow. It has been suggested that the appropriate factor lies between 0.2–0.4 (*12*). In this study, a reduction factor of 0.3 was adopted to scale from blood to marrow. Absorbed-dose calculations for red marrow were performed according to the method of absorbed fractions (*14*).

Needle biopsies, approximately 10 mg in mass, of tumors and normal liver were obtained at 3, 5 or 7 days after the administration of ^{90}Y-CC49. Normal liver biopsies were obtained from 10 patients and tumor biopsies from seven patients. The activity in these samples was measured in the same calibrated gamma counter and channel settings. Activity measurements in tumors and normal liver were subsequently compared to activities computed from ^{111}In-CC49 SPECT scans.

RESULTS

Clearance Characteristics of Indium-111-CC49 and Yttrium-90-CC49 in Tumors and Normal Tissues

The time-activity curves for tumors and normal tissues generated from the analysis of serial gamma camera views, SPECT studies and direct measurements of the activity in tissue samples were described by either monoexponential or biexponential functions. Effective half-lives in tumors, liver, spleen and blood are summarized in Table 1 for the group of 12 patients. In this table, T_α and T_β denote the effective half-lives for the alpha and beta phases, respectively. Tumor uptake in three patients was too low for quantitation by noninvasive imaging. In seven patients, the clearance of ^{111}In-CC49 from tumors was characterized by a monoexponential function. In these patients, maximum tumor uptake was attained at the first imaging time point, less than 2 hr postinjection. In the remaining two patients, the effective half-lives in liver metastases were the same as those for normal liver. Liver and spleen were the only normal organs that could be imaged and had significant uptake and retention of ^{111}In-CC49. In all patients, the activity in normal liver as a function of time postinjection was characterized by an exponential uptake phase that was followed by an exponential clearance phase. The time-course of activity in the spleen was generally characterized by a monoexponential clearance. Maximum splenic uptake was observed at the first imaging time point. The exception was the last patient in Table 1 for whom liver metastasis, normal liver and spleen had the same uptake and clearance characteristics. Clearance of ^{90}Y-CC49 from blood was in all patients characterized by a biexponential function. Additionally, the clearance characteristics of ^{111}In-CC49 and ^{90}Y-CC49 in whole blood were the same. For all patients studied, the effective half-life in tumors was less than or equal to the effective half-life for clearance of activity from the liver.

TABLE 2
Comparison of Measured and Computed Concentrations [kBq/g (μCi/g)] of Yttrium-90-CC49 in Normal Liver Tissue

Patient no.	Measured (biopsy)	Computed (SPECT) [Mean (Range)]	Days*
1	15.2 (0.412)	10.8 (0.291) [5.40–16.9(0.146–0.457)]	7
2	32.6 (0.882)	26.0 (0.703) [15.5–42.9(0.420–1.16)]	7
4	35.7 (0.965)	36.3 (0.981) [8.81–51.1(0.238–1.38)]	5
6	58.5 (1.58)	60.3 (1.63) [37.7–106(1.02–2.86)]	5
7	26.3 (0.710)	33.0 (0.893) [30.4–45.1(0.822–1.22)]	5
8	92.9 (2.51)	92.9 (2.51) [68.1–135(1.84–3.65)]	3
9	64.4 (1.74)	59.6 (1.61) [43.7–64.4(1.18–1.74)]	5
10	88.1 (2.38)	73.6 (1.99) [42.6–94.0(1.15–2.54)]	5
11	58.1 (1.58)	51.4 (1.39) [32.3–74.7(0.873–2.02)]	5
12	40.3 (1.09)	40.0 (1.08) [36.9–44.4(0.996–1.20)]	7

*Number of days postinjection at biopsy.

Comparison of Measured and Computed Concentrations of Yttrium-90-CC49

Measured and computed concentrations of ^{90}Y-CC49 in normal liver tissue are summarized in Table 2 for the 10 patients who had liver biopsies (Patients 3 and 5 had no liver biopsies). With the exception of Patient 7, in this table, measured concentrations in 10-mg needle biopsies were bracketed by the computed ranges of activity concentrations. This table demonstrates the importance of determining the range of values in a VOI when comparing macroscopically computed concentrations with measurements in small-needle biopsies.

Comparison of measured and computed concentrations of ^{90}Y-CC49 in tumor tissue was less conclusive than for normal liver. In part, this was due to the fact that in three patients tumor uptake was too low for SPECT quantitation. However, when SPECT quantitation was possible and tumor biopsies were obtained, measured and computed concentrations compared well in three of four patients. In Patient 6, the measured concentration was 24.1 kBq/g, and the range of computed concentrations was 20.4–25 kBq/g. In Patient 8, the measured and computed concentrations were 17.0 kBq/g and 15.9–20.4 kBq/g, respectively, and in Patient 9 measured and computed activities were 24.4 kBq/g and 26.3–31.8 kBq/g. However, in Patient 7 the measured concentration was 0.37 kBq/g, whereas the range of computed concentrations was 4.81–6.29 kBq/g. It has been shown that the TAG-72 antigen is expressed heterogenously in most adenocarcinomas (*1*). Consequently, macroscopic averages of activity concentrations obtained from SPECT slices can be expected to differ from those measured in small-needle biopsies. Additionally, biopsies were obtained several days after the administration of ^{90}Y-CC49 (Table 2). As the clearance of radioactivity from tumors and normal tissues was described by exponential functions, small errors in half-life determinations would result in a more significant error at late times postinjection.

Time-activity curves of ^{90}Y-CC49 in tumor and normal liver of Patient 6 are shown in Figure 1. This figure illustrates the exponential extrapolations from the time of imaging to the time of biopsy. It also shows the effects of differences in pharmacokinetics on absorbed dose. The initial activity concentration

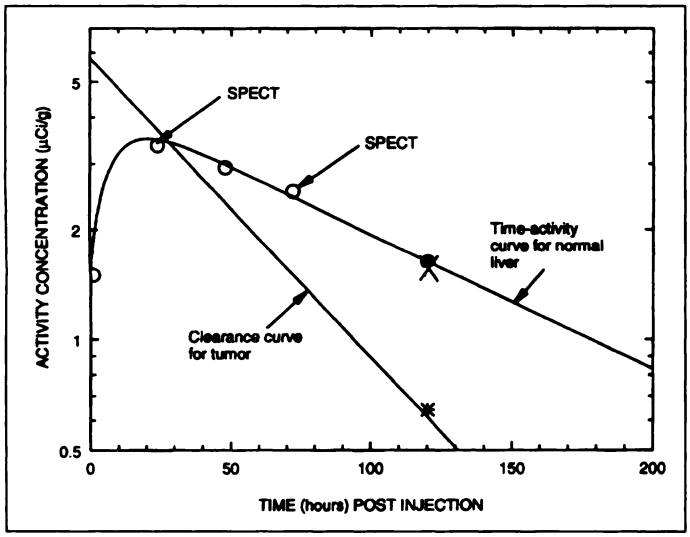

FIGURE 1. Activity concentration of ^{90}Y-CC49 in tumor and normal liver as a function of time postinjection for Patient 6. The open circles denote whole-body imaging at 1, 24, 48 and 72 hr; SPECT studies were acquired at 24 and 72 hr for tumor and normal liver. The time-activity curves show mean values; the range of activity concentrations is given in Table 2 and in the text. The closed circle at 120 hr postinjection is the calculated and X the measured ^{90}Y-CC49 activity concentration in the liver; * indicates the measured ^{90}Y-CC49 tumor concentration.

in this patient's tumor was higher than in normal liver. However, the absorbed dose in the tumor was less than in normal liver because of the shorter effective half-life in the tumor.

Radiation Absorbed-Dose Estimates

Liver and spleen were the only normal organs that had measurable and significant uptake and retention of ^{111}In-CC49. Administered activities of ^{90}Y-CC49 and absorbed-dose estimates for tumors, liver, spleen and red marrow for the 12 patients studied are summarized in Table 3. For tumors, liver and spleen calculations were image-based and include the mean and range of values. Absorbed-dose estimates for red marrow were based on time-activity measurements of ^{90}Y-CC49 in blood and, hence, are given by single numbers.

Tumor uptake of ^{90}Y-CC49 was less than or equal to that of normal liver and this is reflected in the dose calculations. An encouraging observation was that increases in administered activity were accompanied by increases in the absorbed dose in tumors. However, the absorbed dose in liver and spleen also increased as the administered activity was increased. In contrast, the absorbed dose in red marrow remained nearly constant as the administered activity was increased from 11.1 MBq/kg to 18.5 MBq/kg.

DISCUSSION

Although the conjugate-view method for activity quantitation from planar gamma camera views is still widely used (*15,16*), this method suffers from several shortcomings as has been detailed elsewhere (*5*). Planar gamma camera views do not provide the volumetric information that is usually needed for dosimetry and they do not provide sufficient information about the distribution of activity within an organ or tumor. Only a mean value of activity can be obtained from planar gamma camera views and, hence, only a mean value of radiation absorbed dose can be calculated. These difficulties can be overcome with emission-tomographic methods, and SPECT has been used by several investigators for the quantitation of activity (*8–10,17–20*).

The emphasis of this report is on radiation dosimetry and the underlying comparison of measured and computed activity concentrations. We have demonstrated in this study that SPECT quantitation of ^{111}In-CC49 can be used successfully to compute ^{90}Y-CC49 concentrations in tumors and normal liver. This finding was important because radiation absorbed-dose estimates for tumors, liver and spleen were, to a large extent, based on quantitative imaging of ^{111}In-CC49. Although no spleen biopsies were obtained, we have included absorbed-dose estimates for this organ (Table 3) because it had significant uptake of ^{111}In-CC49. It was, therefore, important to estimate the absorbed dose for the spleen. In making these estimates, it was assumed that the pharmacokinetics of ^{111}In-CC49 and ^{90}Y-CC49 were identical in the spleen. Determination of the distribution of activity proved essential for making a meaningful comparison of macroscopically computed activities with measured activities in small-needle biopsies. Additionally, SPECT acquisitions at 24 and 72 hr postadministration of ^{111}In-CC49 showed that there was no redistribution of radiolabeled antibody in this time interval. In conjunction with planar whole-body imaging and tissue biopsies obtained 3–7 days postadministration of ^{90}Y-CC49, this provided justification for using effective half-lives beyond the imaging time points in making radiation absorbed-dose estimates. In absorbed-dose estimates, we have ignored bremsstrahlung radiation because in soft tissue only about 1% of the beta-particle energy is converted to bremsstrahlung. Consequently, in source tumors and normal organs, the bremsstrahlung absorbed dose is negligibly

TABLE 3
Administered Activities of Yttrium-90-Labeled CC49 and Radiation Absorbed-Dose Estimates (cGy)

Patient no.	MBq (mCi) administered	Tumor		Liver		Spleen		Marrow
		Mean	(Range)	Mean	(Range)	Mean	(Range)	Mean
1	640 (17.3)	570	(130–1180)	370	(190–570)	670	(540–1060)	70
2	844 (22.8)	NA	NA	720	(430–1190)	580	(370–850)	74
3	881 (23.8)	360	(280–410)	580	(220–990)	0	0	72
4	914 (24.7)	600	(530–720)	420	(100–590)	460	(170–680)	50
5	929 (25.1)	NA	NA	600	(370–900)	700	(550–1060)	50
6	1062 (28.7)	610	(550–680)	850	(530–1490)	800	(730–910)	64
7	1051 (28.4)	200	(170–230)	720	(660–990)	410	(380–460)	56
8	1151 (31.1)	970	(910–1070)	890	(650–1290)	750	(690–930)	88
9	1277 (34.5)	2400	(2190–2580)	2400	(1760–2580)	800	(670–910)	57
10	1354 (36.6)	NA	NA	750	(440–960)	440	(300–640)	60
11	1421 (38.4)	1100	(1000–1250)	2900	(1820–4220)	2400	(1820–3000)	120
12	1373 (37.1)	3000	(2660–3340)	3000	(2770–3330)	2100	(1790–2340)	82

NA = not available; tumor uptake was too low for quantitation by imaging.

small compared to the beta dose. Additionally, for the administered activities of ^{90}Y-CC49 used in this study and concentrations achieved, the bremsstrahlung absorbed dose in other organs was < 1 cGy (*21*). We also have ignored the absorbed dose resulting from the administration of the tracer activity of ^{111}In-CC49. This activity was much lower than that of ^{90}Y-CC49, and the physical properties of ^{111}In are such that in this study ^{111}In provided an insignificant absorbed dose per unit cumulated activity in source organs in comparison with ^{90}Y (*22*).

It is important to note that up to 90 cGy/mCi were deposited in tumors (Table 3). This was considerably higher than previously reported for other radiolabeled monoclonal antibodies (*15,16*). This supports the continued study of ^{90}Y-CC49. However, the finding of equally high activity concentrations in tumors and normal liver mandates alternate approaches to either preferentially increase the absorbed dose in tumors over that in normal liver or decrease the absorbed dose in normal liver.

The estimate of the maximum absorbed dose of 3,300 cGy in normal liver (Table 3) was well within the generally accepted limit of 3,000–3,500 cGy for external-beam therapy (*23,24*). It was also in the same range as the absorbed dose in normal liver reported for ^{131}I-lipiodol therapy of hepatomas (*25*). In that trial, the normal-liver dose ranged from 200–3,800 cGy. Considerably higher absorbed doses in normal liver have been reported for ^{90}Y microspheres administered through the hepatic artery for the treatment of hepatoma. Normal-liver doses up to about 8,900 cGy (*26*) and 15,000 cGy (*27*) were tolerated without causing hepatic toxicity. There is, thus, an increasing body of clinical evidence which suggests that the exponentially decreasing low dose-rate irradiation of normal liver by ^{90}Y beta particles is significantly less toxic than high dose-rate external-beam irradiation.

CONCLUSION

The comparison of measured and computed activity concentrations in tumors and normal tissues has demonstrated that quantitative imaging of ^{111}In-CC49 PA-DOTA is valid for patient-specific dosimetry of ^{90}Y-CC49 PA-DOTA. By extracting ranges of activity concentrations from sets of transverse SPECT slices, we were able to compute a mean value and range of absorbed dose for tumors, liver and spleen. This provided a more complete description of absorbed dose than has been achievable with planar gamma camera conjugate-view methods (*4,15,16*).

ACKNOWLEDGMENTS

This work was supported in part by National Cancer Institute grant U01 CA58272 and Department of Energy grant FG02–91ER61195. A preliminary account of this work was presented at the 43rd Annual Meeting of the Society of Nuclear Medicine in Denver, CO, in June 1995.

REFERENCES

1. Esteban JM, Colcher D, Sugarbaker P, et al. Quantitative and qualitative aspects of radiolocalization in colon cancer patients of intravenously administered MAb B72.3. *Int J Cancer* 1987;39:50–59.
2. Divgi CR, Scott AM, Cantis L, et al. Phase I radioimmunotherapy trial with ^{131}I-CC49 in metastatic colon carcinoma. *J Nucl Med* 1995;36:586–592.
3. Murray JL, Macey DJ, Kasi LP, et al. Phase II radioimmunotherapy trial with ^{131}I-CC49 in colorectal cancer. *Cancer* 1994;73:1057–1066.
4. Leichner PK, Yang N-C, Frenkel TL, et al. Dosimetry and treatment planning for Y-90 labeled antiferritin in hepatoma. *Int J Radiat Oncol Biol Phys* 1988;14:1033–1042.
5. Leichner PK, Koral KF, Jaszczak RJ, Green AJ, Chen GTY, Roeske JC. An overview of imaging techniques and physical aspects of treatment planning in radioimmunotherapy. *Med Phys* 1993;20:569–577.
6. Cheng R, Fordyce WA, Goecklerer WF, et al. Macrocyclic conjugates and their use as diagnostic and therapeutic agents. U.S. Patent 5,435,990; 1995.
7. Schott ME, Schlom J, Siler K, et al. Biodistribution and preclinical radioimmunotherapy studies using radiolanthanide-labeled immunoconjugates. *Cancer* 1994; 73(suppl):993–998.
8. Hawkins WG, Leichner PK, Yang N-C. The circular harmonic transform for SPECT reconstruction and boundary conditions on the Fourier transform of the sinogram. *IEEE Trans Med Ima* 1988;7:135–148.
9. Hawkins WG, Yang N-C, Leichner PK. Validation of the circular harmonic transform (CHT) algorithm for quantitative SPECT. *J Nucl Med* 1991;32:141–150.
10. Leichner PK, Vriesendorp HM, Hawkins WG, et al. Quantitative SPECT for In-111-labeled antibodies in the livers of beagle dogs. *J Nucl Med* 1991;32:1442–1444.
11. Berger MJ. Distribution of absorbed dose around point sources of electrons and beta particles in water and other media. *MIRD pamphlet no. 7*. New York, NY: Society of Nuclear Medicine 1971:7–32.
12. Siegel JA, Wessels BW, Watson EE, et al. Bone marrow dosimetry and toxicity for radioimmunotherapy. *Antibody Immunoconj Radiophar* 1990;3:213–233.
13. Sgouros G. Bone marrow dosimetry for radioimmunotherapy: theoretical considerations. *J Nucl Med* 1993;34:689–694.
14. Whitwell JR, Spiers FW. Calculated beta-ray dose factors for trabecular bone. *Phys Med Biol* 1976;21:16–38.
15. Breitz HB, Fisher DR, Weiden PL, et al. Dosimetry of Re-186-labeled monoclonal antibody: methods, prediction from Tc-99m-labeled antibodies and results of Phase I trials. *J Nucl Med* 1993;34:908–917.
16. Breitz HB, Durham JS, Fisher DR, et al. Pharmacokinetics and normal organ dosimetry following intraperitoneal Re-186-labeled monoclonal antibody. *J Nucl Med* 1995;36:754–761.
17. Green AJ, Dewhurst SE, Begent RH, Bagshawe KD, Riggs SJ. Accurate quantification of ^{131}I distribution by gamma camera imaging. *Eur J Nucl Med* 1990;16:361–365.
18. Israel O, Iosilevsky G, Front D, et al. SPECT quantification of I-131 concentration in phantoms and human tumors. *J Nucl Med* 1990;31:1945–1949.
19. Gilland DR, Jaszczak RJ, Greer KL, Coleman RE. Quantitative SPECT reconstruction of I-123 data. *J Nucl Med* 1991;32:527–533.
20. Gilland DR, Jaszczak RJ, Turkington TC, Greer KL, Coleman RE. Quantitative SPECT imaging with In-111. *IEEE Trans Nucl Sci* 1991;32:761–766.
21. Stabin MG, Eckerman KF, Ryman JC, Williams LE. Bremsstrahlung radiation dose in Y-90 therapy applications. *J Nucl Med* 1994;35:1377–1380.
22. Snyder WS, Ford MR, Warner GG, Watson SB. "S," absorbed dose per unit cumulated activity for selected radionuclides and organs. *MIRD pamphlet no. 11*. New York: Society of Nuclear Medicine; 1975:144–145, 164–165.
23. Ingold J, Reed G, Kaplan H, Bagshaw M. Radiation hepatitis. *Am J Roentgenol* 1965;93:200–208.
24. Lewin K, Millis R. Human radiation hepatitis. *Arch Path* 1973;96:21–26.
25. Raoul JI, Bretagne JF, Cancanas JP, et al. Internal radiation therapy for hepatocellular carcinoma: results of a French multicenter Phase III trial of transarterial injection of I-131 labeled lipiodol. *Cancer* 1992;69:346–352.
26. Gray BN, Burton MA, Kelleher D, Klemp P, Metz L. Tolerance of the liver to the effects of Y-90 radiation. *Int J Rad Oncol Biol Phys* 1990;18:619–623.
27. Andrews JC, Walker SC, Ackermann RJ, Cotton LA, Ensminger WD, Shapiro B. Hepatic radioembolisation with Y-90 containing glass microspheres: preliminary results and clinical follow-up. *J Nucl Med* 1994:1637–1644.